Available online at http://scik.org

Commun. Math. Biol. Neurosci. 2026, 2026:53

https://doi.org/10.28919/cmbn/9886

ISSN: 2052-2541

COMBAT HARMONIZATION OF RS-FMRI IMPROVES CLASSIFIER PERFORMANCE IN PATIENTS WITH AUTISM SPECTRUM DISORDER: A GRAPH THEORETICAL APPROACH

ANOOP JACOB THOMAS*, V. KIRAN RAJ

Department of Computer Science & Engineering, Indian Institute of Information Technology Tiruchirappalli, India

Abstract: Resting state functional connectivity is identified to reflect the intrinsic organization of the brain's cognitive characteristics. One key property of such biological networks is modularity. In this paper, an open dataset ABIDE of which a total of 45 ASD (Autism Spectrum Disorder) and 53 TD (Typical Development) participants from KKI and PITT sites was considered. Graph Theoretic measures involving Degree Centrality, Clustering Coefficient and Modularity were calculated at different thresholds of network connectivity. Linear SVM classifiers were used to distinguish between ASD and TD. The classifier was applied to each of these graph measures at individual threshold levels. Further, ComBat harmonization across both sites was performed to which the above classification model was applied. Experimental results show that participants from KKI sites showed a difference in Newman modularity at 0.3 threshold with 76.1% accuracy with specificity and sensitivity of 73.08% and 81.25% respectively. Although the accuracy of the site-specific TD vs ASD classifiers were comparable, the sensitivity of the KKI classifier was less, which improved post harmonization. Similar performance was observed in degree centrality and clustering coefficient measures. Therefore, the harmonization process plays a significant role in classifier performance and in model selection.

Keywords: rsfmri; functional connectivity; graph measures; combat; svm.

2020 AMS Subject Classification: 62H30, 92C42, 68R10, 92C55.

*Corresponding author

E-mail address: anoopjt@iiitt.ac.in

Received March 19, 2026

1. INTRODUCTION

Autism Spectrum Disorder (ASD) involves a neurological condition which is associated with disorders in cognitive abilities, Cognitive abilities such as speech, motor coordination and other social activities can be affected in patients diagnosed with ASD. This neurological condition mainly affects children or adolescents caused due to genetic and environmental factors. There is a steady rise in the prevalence of ASD in Asia resulting in a worrying trend over the last decade, S. Qiu et. al [1] and N. Salari et. al [2]. However, early prognosis and intervention for these patients can significantly improve their condition in the long term.

Human cognition and neurological disorders are mainly discovered through neural underpinnings which involve the structure and function of the brain. These neural underpinnings are identified as brain connectivity patterns which are computed as statistical/causal dependencies among other parameters known as functional connectivity which can be characterized through graph measures such as clustering coefficient, modularity, etc., F. V Farahani et. al [3]. From the different types of neuroimaging modalities, the resting state functional MRI (rsfMRI) is a preferred method to study the fluctuations in the Blood Oxygenation Level Dependent (BOLD) response which reflects certain cognitive characteristics that can be analyzed through functional connectivity, M. A. Just et. al [4]. This connectivity measures the coherence between two or more defined brain regions at a specific instant of time. Each of such regions is defined by an averaged intensity over a predefined anatomical region.

Many studies have revealed that functional connectivity patterns have been used in the development of biomarkers in many disorders such as Depression, Parkinson's Disease and Attention Deficit Hyperactivity Disorder (ADHD). However, one of the major limitations of functional connectivity measures is that of reproducibility and generalizability. While studies identify that patients with ASD exhibit reduced long distance connectivity, such patients can also exhibit hypo and hyper connectivity, L. Borràs-Ferrís et. al [5], H. Haghighat et. al [6], J. Xu et. al [7] and Z. K Khadem-Reza et. al [8].

Although recent developments in machine learning and deep learning techniques have been

effective in classifying neurological conditions from healthy controls G. Deshpande et. al [9], G. Deshpande et. al [10], M. K. Belmonte et. al [11] and A. A. Chen et. al [12], the issue of generalizability of neural correlates among these patients is still an active area of research, A. Di Martino et. al [13]. Some of the likely confounds that could affect the classifier performance, Y. Du et. al [14] involve systematic artifacts, methodological heterogeneity and subject heterogeneity, many of these factors lead to batch effects causing multisite variability, To address this issue harmonization frameworks for functional MRI are developed, M. N. Hallquist and F. G. Hillary [15], R. K. Kana et. al [16] and A. Khazaee et. al [17]. Further, the process of harmonization can influence the classifier performance in many instances, N. Masuda et. al [18].

In this study, patients with ASD are differentiated from TD (Typical Development) using graph theoretic measures of functional connectivity involving centrality and modularity measures. The study further identifies if harmonizing fMRI data of the same pathology from different acquisition sites with differing acquisition protocols affects the classifier performance.

The paper is structured as follows, an introduction on graph measures derived from functional connectivity measures is provided. Further, the proposed methodology explains the computation of graph measures from preprocessed fMRI which is then harmonized across multiple sites. Further, graph measures are evaluated through a support vector machine during pre and post harmonization process in classifying ASD from Typical Development participants.

2. METHODOLOGY

2.1. DATASET DESCRIPTION

The ABIDE (Autism Brain Imaging Data Exchange) dataset is used in this study, A. Di Martino et. al [13]. Resting state fMRI of ASD (Autism Spectrum Disorder) and TD (Typical Development) across KKI (Kennedy Krieger Institute) and PITT (University of Pittsburgh school of Medicine) sites are analyzed for this study. A total of 20 ASD and 28 TD participants were acquired from KKI site, followed by 29 ASD and 27 TD participants from PITT site. The mean age among ASD and TD across KKI are 10 ($\pm$ 1.4) and 10 ($\pm$ 1.3) years respectively. Among these participants, the ASD population constitutes 16 male and 4 female participants, TD population constitutes 20

male and 8 female participants. Similarly, the mean age of ASD and TD across PITT are 19 (± 7.0) and 18 (± 6.4) years respectively. Among these participants, the ASD population constitutes 25 male and 4 female participants, TD population constitutes 23 male and 4 female participants. Post harmonization process, the participants from KKI and PITT sites were combined resulting in a total of 45 ASD and 53 TD participants.

2.2. PREPROCESSING OF RESTING STATE FUNCTIONAL MRI

The Preprocessing of the functional MRI was performed as per the methodology stated in this study V. K. Raj et. al [56], However, the current study focuses on PITT and KKI sites which acquired the rsfMRI scans from Siemens Magnetom Allegra Syngo MR A30 and Philips Achieva 3.0T for 5.06 and 6.40 minutes respectively. The Repetition time for PITT and KKI was 1500ms and 2500 ms with slice thickness of 4mm and 3mm respectively. Further, To identify the low frequency components, a bandpass filter of 0.01 to 0.1 Hz was applied. The resulting averaged time series for each anatomical region (AAL atlas, N. Tzourio-Mazoyer et. al [26]) is then extracted from the preprocessed rsfMRI scans yielding a 90 x 152 matrix (regions x scans) for each subject for KKI and 90 x 196 for PITT sites respectively. Further, Pearson correlation is computed across the anatomical regions resulting in a 90 x 90 matrix for each subject for each threshold value (fig. 1).

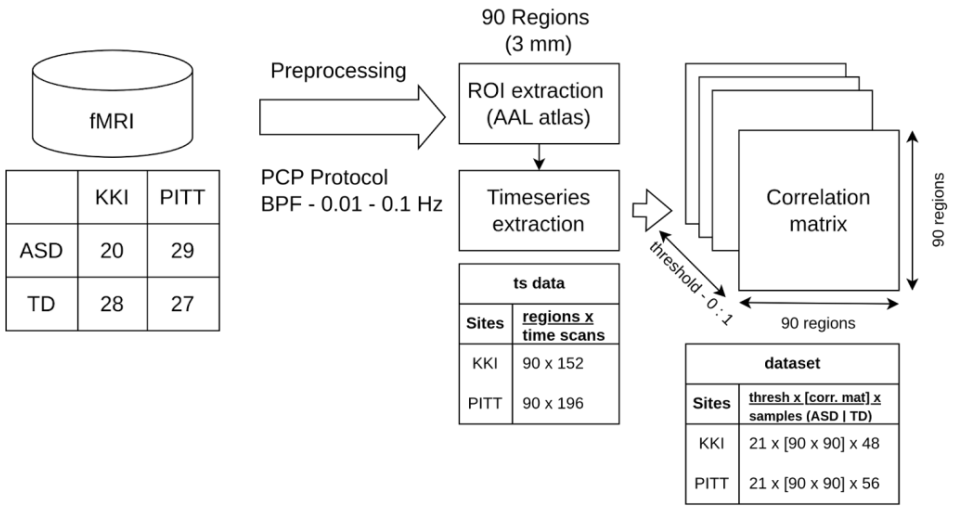

Figure 1: fMRI preprocessing and FC construction

2.3. Constructing Functional Connectivity for Graph Theoretical Measures

Among many representations of the functional MRI such as Independent Component Analysis (ICA), Regional Homogeneity (ReHo), Amplitude of Low Fluctuation Frequency (ALFF), M. E. J. Neuman and M. Girvan [21] and K. Qin et. al [22]. Graph theoretical measures interpret the neurological disorder as a network disorder. A concept which is important in ASD diagnosis K. Rajamanickam [23].

The resulting 90 x 90 correlation matrix represents the functional connectivity of the whole-brain network for each subject, where each ROI (Region of Interest) is identified as a network node and the correlation strength as measure of connectivity among these nodes, E. Redcay et. al [24]. The correlation strength quantifies the relationship between the time-series of two ROIs. Once such a matrix is constructed for whole-brain network, various methods are used to express the relation of these nodes in terms of graph measures. In this context, the adjacency matrix required for graph computation is developed considering the ROI as nodes and correlation strength as edges resulting in weighted undirected 90 x 90 adjacency matrix for each participant. Further, such an adjacency matrix is thresholded by absolute weight ranging from 0 to 1 with an increment of 0.05. Therefore, 0 threshold represents all edges with minimum correlation strengths between ROIs, and 1 represents all edges with maximum correlation strengths between ROIs, leading to 21 adjacency matrices for each participant.

Graph theoretical analysis involving centrality measures and modularity were performed for all 21 adjacency matrices for each participant across both the sites (fig. 2). Measures such as degree centrality, clustering coefficient and modularity S. Hiwa et. al [25] are calculated resulting in a 1 x 90 vector for each graph measure, where each ROI's relation to the rest of the ROI's are characterized by these measures V. K. Raj et. al [56]. The graph computation was performed using the Brain Connectivity Toolbox, Matlab, M. Rubinov and O. Sporns [29].

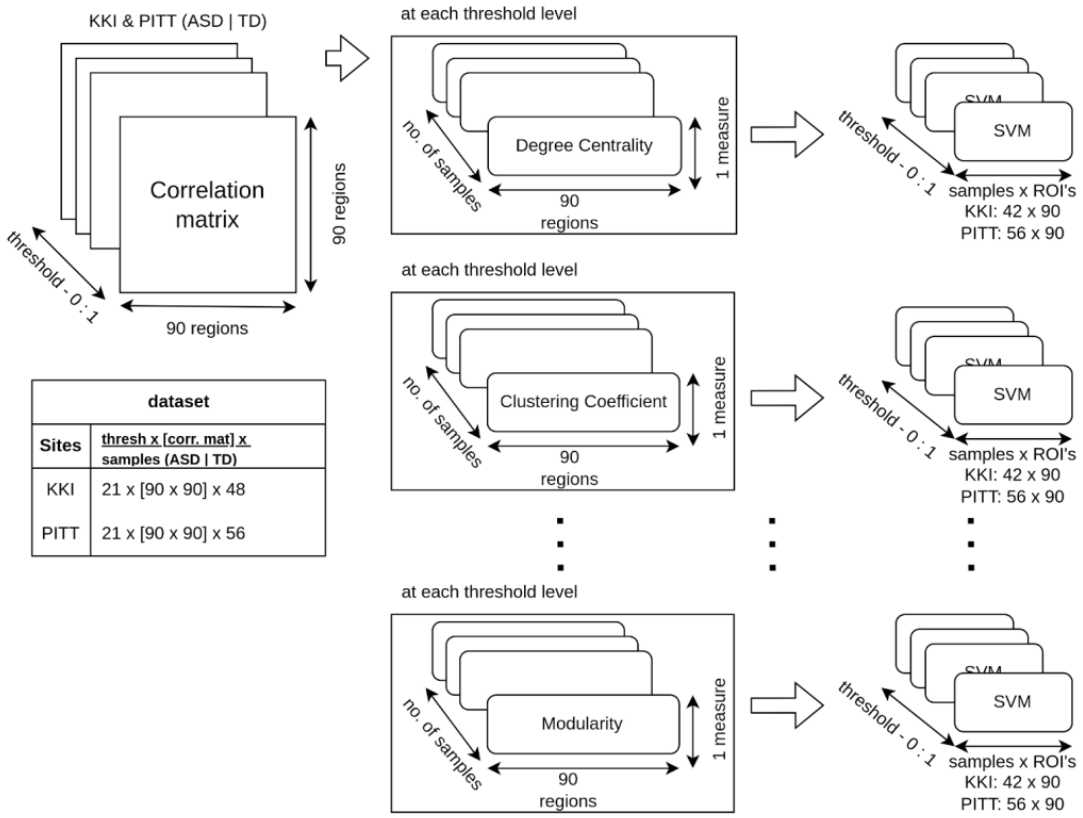

Figure 2: Graph theoretical measures

The graph measures computed in this study is illustrated as follows.

Clustering coefficient: The local clustering coefficient which was originally proposed by J. P. Onnela et. al 2004 [27] was further developed by M. Rubinov and O. Sporns [29] which is defined in (1) as follows:

$$C_i^{wei,O} = \frac{1}{k_i(k_i-1)} \sum_{1\le j,l\le N_{ROI}, j,l\neq i} \frac{(w_{i,j}w_{i,l}w_{j,l})^{\frac{1}{3}}}{max_{i',j'}w_{i',j'}} \quad (1)$$

where, $C_i^{wei,O}$ →average global clustering coefficient, i,j, l → nodes that form a triangle; w→ weights of the nodes; k_i→ sum of all edges to node i (also known as degree centrality of node i)

Modularity: Modularity measures play a significant role in many functional characteristics of the brain. Factors such as brain evolution, wiring cost and creation of specialized information and complex dynamics involve modularity measures M. Rubinov and O. Sporns [29] and O. Sporns et. al [30]. Considering the network to be organized as “modules”, graph-partioning based problems

were popularized by M. E. J. Newman and Girvan [21] which is defined as follows (2)

$$Q = \frac{1}{2m} \sum_{C \in P} \quad \sum_{i,j \in C} \quad \left[A_{ij} - \frac{k_i k_j}{2m} \right] \tag{2}$$

where, A→Adjacency matrix. m→total number of edges and k_i→degree of node i, C→index which runs over modules of partition P. Recent methods involved decomposing the network into submodules at a hierarchical level called as Louvain Modularity. It consists of two phases, the first phase selects nodes sequentially in an order that has been randomly assigned, the second phase builds a new network whose nodes are communities identified in the first phase, V. D. Blondel et. al [31] and D. Meunier et. al [19].

At this stage, two models are implemented (fig. 3), the first model is performing classification between ASD and TD for each site across all threshold levels. The second model is performing classification between ASD and TD after harmonizing graph measures across sites at each threshold level L. Q. Uddin et. al [34]. Linear Support Vector Machine (SVM) was implemented for classification with 10 fold cross validation while maintaining the same data folds across all thresholds. The classifier performance for each model is validated using sensitivity and specificity measures.

2.4. COMBAT HARMONIZATION ON GRAPH MEASURES

In this study, the ComBat based harmonization method was used which is known to reduce the potential biases and non-biological variability which are induced by site and scanner effect, M. Eshaghzadeh Torbati et. al [33]. This method uses a multivariate linear mixed effects regression to model the imaging feature measurements. The ComBat harmonizes mean variances of residuals across different batches, which is known as Location-Scale harmonization. No biological covariates (age, gender, etc.) are set during harmonization as only two sites are considered in this study. Studies have shown ComBat substantially reducing scanner effects in metrics such as global efficiency, local efficiency and community measures, M. Yu et. al [57]. The harmonization process which is based on the scale and shift regression is shown in (3):

$$Y = X\beta + S\beta_* + ((S\delta) \cdot \epsilon) \tag{3}$$

where, Y→regression output, S→design matrix which remains consistent for all batches β_*→site mean and variance; δ→ multiplicative scale changes.

In context of functional connectivity, ComBat (Functional Connectivity) assumes scanner effects influence all edges similarly and uses empirical bayes estimation method to borrow information across all edges. The advantage of ComBat harmonization is its robustness towards outliers in small batch sizes which is prevalent in the present study. Post the harmonization of each graph measure across KKI and PITT sites, Linear SVM classification was performed to distinguish between ASD from TD across all threshold levels.

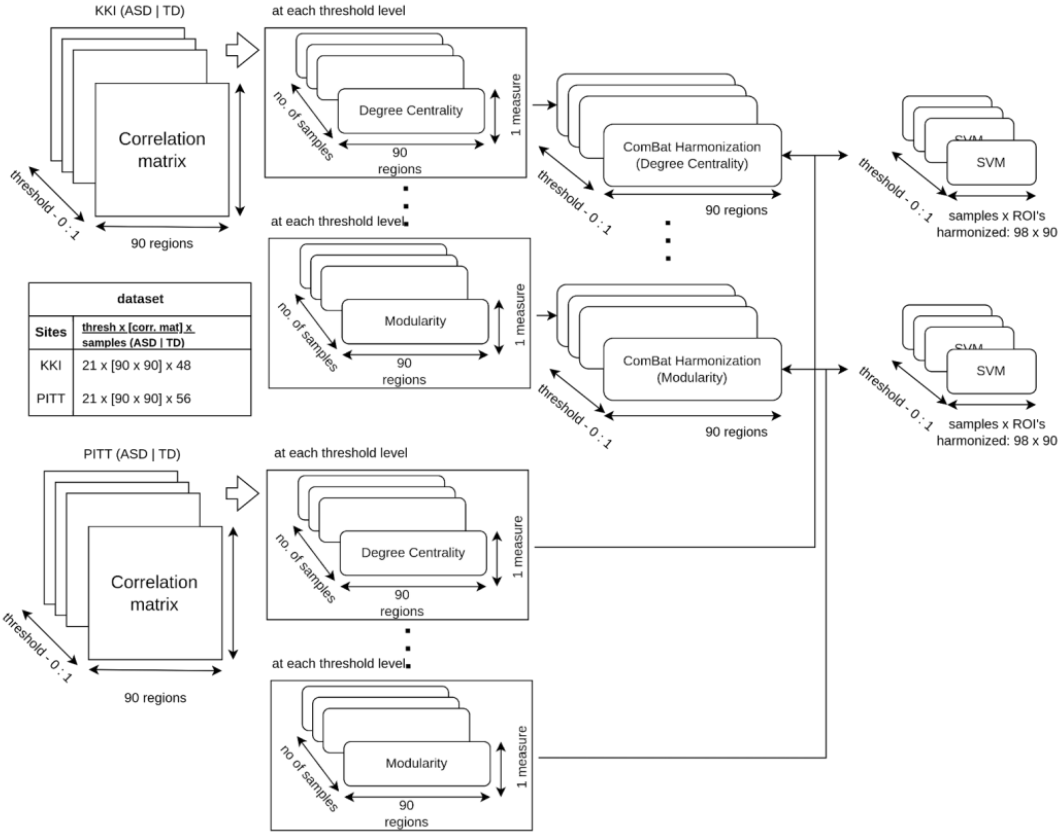

Figure 3: Harmonization of graph measures

2.5. CLASSIFICATION

As mentioned earlier, classification is performed prior to and post harmonization of graph measures. Prior to harmonization process, a total of 48 samples were considered from KKI site which constitutes 20 ASD and 28 TD participants, of these 4 and 2 samples were identified as

outliers in ASD and TD respectively, resulting in a total of 42 samples. Four graph measures were computed involving degree centrality, clustering coefficient, Louvian and Newman modularity, resulting in 4 x 42 x 90 matrices (graph measure x samples x ROIs) for a total of 21 threshold levels. Similarly, a total of 56 samples were considered from PITT site which constitutes 29 ASD and 27 TD participants for which the above four graph measures were computed resulting in 4 x 56 x 90 x 21 matrices. Post harmonization, a total of 98 samples was considered for classification, which included 45 ASD and 53 TD participants from both KKI and PITT sites resulting in 4 x 98 x 90 x 21 matrices. All the above models were then validated individually using a k-fold cross validation (where, k=10) through the confusion matrix yielding sensitivity and specificity measures to distinguish ASD from TD participants.

3. MAIN RESULTS

3.1. RELATION BETWEEN THE NETWORK EDGES AND THRESHOLD LEVELS

The methodology for analyzing the number of edges was performed as per the methodology performed in this study, V. K. Raj et. al [56] for PITT and KKI sites with ~4000 edges remained the same upto a 0.25 threshold for both ASD and TD. The number of edges were inversely proportional to the threshold. Among the two sites, the KKI site for both groups showed a comparatively lower number of edges (fig.4).

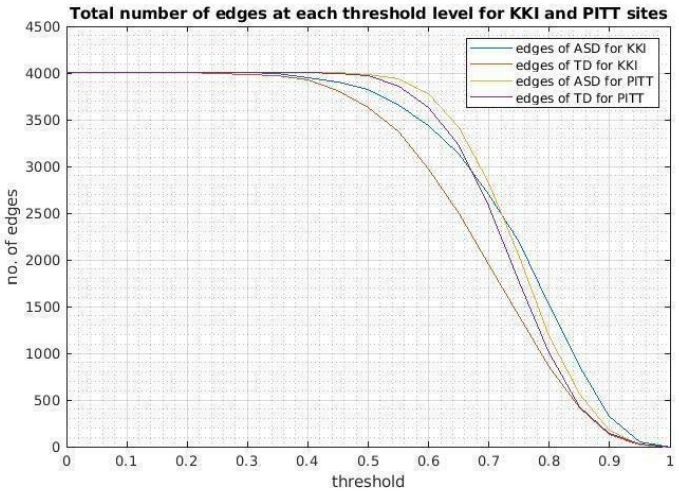

Figure 4: Number of edges at each threshold level for KKI, PITT and post harmonization

3.2. Classifier Performance for Graph Measures for KKI, PITT and Post Harmonization

Graph theoretical measures such as degree centrality, clustering coefficient, Louvian and Newman modularity were computed at each threshold level with an interval of 0.05. The degree centrality for ASD and TD participants were identified as the number of neighbors connected to a specific ROI. Modularity measure parcellates each functional network into sub-groups that are highly interconnected among themselves as compared to the rest of the network. The presence of such highly connected sub-groups is known as "community structure" M. Rubinov and O. Sporns [29]. The Louvain and Newman modularity are computed for both KKI and PITT sites for ASD and TD participants. The advantage of modularity measures in fMRI is that modules can be detected from a purely data-driven approach based on the network topology, V. D. Blondel et. al [31]. Each ROI was associated with a minimum of 1 group to a maximum of 4 groups across all sites and conditions. Another approach towards modularity detection proposed by M. E. J. Newman et. al [20] was calculated, which mainly reduces the influence of random factors in a network, resulting in a community affiliation vector of 1 x 90 for each participant across KKI and PITT sites. A Linear SVM (Support Vector Machine) is applied to each of these graph measures for KKI and PITT sites to distinguish ASD from TD participants with a 10 fold cross validation.

In the second model, the graph measures from both the KKI and PITT sites are harmonized independently for ASD and TD using the ComBat harmonization, resulting in a dataset of size 98 x 90 (45 ASD; 53 TD and graph measures for 90 ROI's) at all threshold levels.

As observed from the above fig 5, the accuracy for degree centrality has increased for both KKI and PITT sites for higher thresholds, Although, the accuracy for clustering coefficient had initially decreased, an increasing trend was observed post a threshold of 0.5. For both the measures, the behavior of the classifier performance post harmonization remained consistent with that of the individual sites. Similarly, for Louvain and Newman modularity (fig. 6) observed a decreasing trend in distinguishing between ASD from TD with a declining accuracy in KKI and PITT sites, a

similar behavior was observed post harmonization for both the measures.

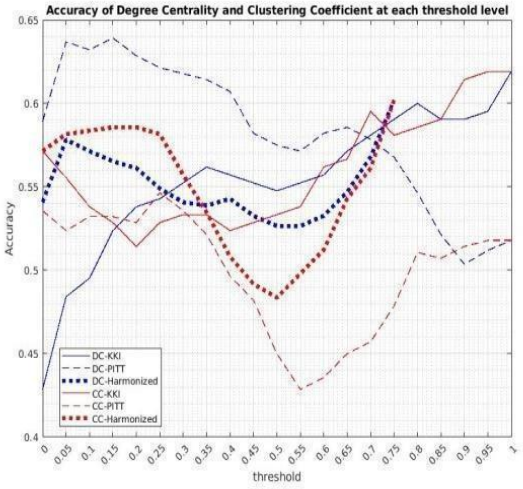

Figure 5: Accuracy* of DC and CC

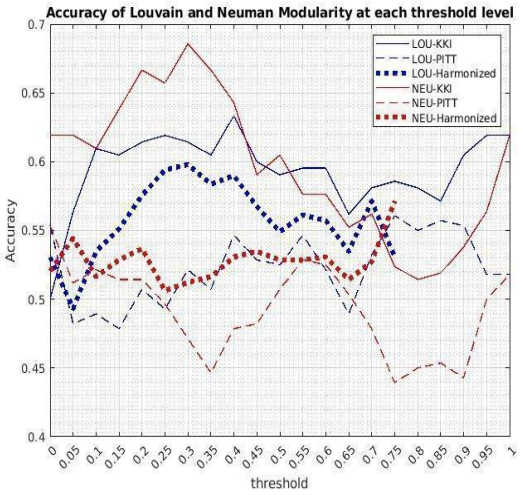

Figure 6: Accuracy* of Modularity Measures

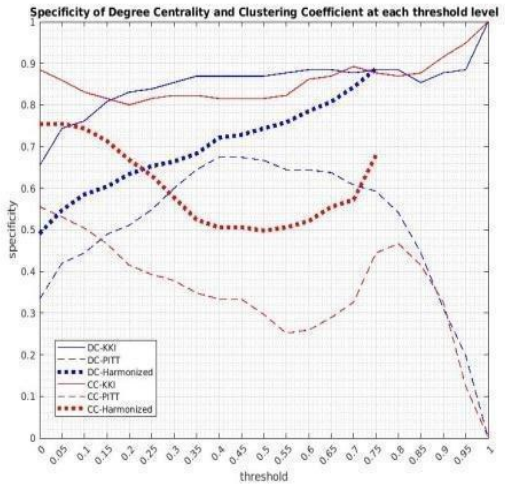

Figure 7: Specificity* of DC and CC

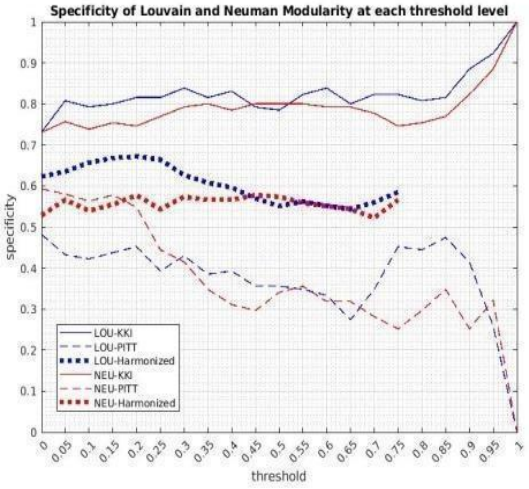

Figure 8: Specificity* of Modularity Measures

*values are smoothened using moving average across threshold levels

The specificity remained consistently higher even when total edges for ASD and TD decreased to 327 and 133 respectively. i.e., the number of edges in TD decreased more than 25% compared to ASD at this threshold and continued to decrease upto 58.8 % at a threshold value of 0.9. However, the specificity of the PITT site did not observe a similar behavior compared to KKI. Interestingly, there is a sharp decline in specificity from threshold value ranging from 0.7 to 1 (also indicated in table 1), even though the number of edges were similar to KKI site at 0.7 threshold

(ASD=2821;TD=2576). Post harmonization, both degree centrality and clustering coefficient showed a consistent increase in specificity with increasing threshold value greater than 0.4 (fig. 7), while also observing improved sensitivity (table. 1).

Table 1: Classifier Performance Post Harmonization

Classifier performance post harmonization

	Th	ACC	SPC	SEN	TN	FP	FN	TP
DC_KKI	0.9	61.9	88.4	18.7	23	3	13	3
DC_PITT	0.7	66.0	74.0	58.6	20	7	12	17
DC[1]	**0.7**	**60.2**	**88.6**	**26.2**	**47**	**6**	**33**	**12**
CC_KKI	0.8	66.6	92.3	25.0	24	2	12	4
CC_PITT	0.9	55.3	29.6	79.3	8	19	6	23
CC[1]	**0.7**	**60.2**	**67.9**	**51.1**	**36**	**17**	**22**	**23**
LOU_KKI	0.2	69.0	88.4	37.5	23	3	10	6
LOU_PITT	0.5	69.6	59.2	79.3	16	11	6	23
LOU[1]	**0.2**	**65.3**	**67.9**	**62.2**	**36**	**17**	**17**	**28**
NEU_KKI	0.3	76.1	73.0	81.2	19	7	3	13
NEU_PITT	0.5	67.8	48.1	86.2	13	14	4	25
NEU[1]	**0.1**	**62.2**	**69.8**	**53.3**	**37**	**16**	**21**	**24**

[1]→ Post Harmonization

A similar trend was observed for Louvain modularity measures for both sites, however, post harmonization, the specificity remained consistent across increasing threshold levels. As observed from table 1, highest accuracy post harmonization was identified at 0.2 and 0.1 threshold in Louvain and Newman modularity with 65.31% and 62.24% respectively. Although the overall classifier performance for modularity measures declined post harmonization, it achieved a comparatively improved specificity while sensitivity in Newman modularity declined. However, an increasing trend in sensitivity was observed in degree centrality, clustering coefficient and

Louvain Modularity measures post harmonization at threshold ranging from 0.7 - 0.9 (for centrality measures) respectively (when compared to KKI site).

4. DISCUSSION

4.1. ASD CHARACTERIZATION THROUGH FUNCTIONAL CONNECTIVITY

Studies reveal predominant under-connectivity in long-range connections J. D Rudie et. al [35], especially within the default mode network (DMN) involving regions like the medial prefrontal cortex and posterior cingulate cortex, linked to social cognition deficits. Over-connectivity appears in local or short-range links S. Achard and E. Bullmore [37], such as increased regional homogeneity (ReHo) in severe ASD subtypes, alongside atypical connections in sensorimotor and salience networks. Both hypo- and hyper-connectivity contribute to heterogeneity, contributing to the social, cognitive and behavioral abnormalities presented by such patients J. D. Rudie et. al [35], D. S. Bassett and E. Bullmore [36] and S. Achard and E. Bullmore [37].

As observed from the present study, the centrality measures such as degree centrality and clustering coefficient play a significant role in distinguishing ASD from TD, a finding which is similar to J. R. Sato et. al [38]. This study further reinforced the underconnectivity that was identified in ASD patients which explains the overall decrease in accuracy considering modularity measures alone (fig.4(b)). However, the complexities of these networks are captured more evidently through modularity measures when considering the specificity between ASD and TD, Here, the two sites showed a contrasting trend, i.e., while specificity of KKI increased with the increasing threshold value, scans acquired from the PITT site showed the classifier model yielding reduced sensitivity over the same threshold range. This contrasting trend could be the possible effect of site variability among KKI and PITT sites as evidently observed from the above findings. This leads to the requirement of harmonization among different sites. This is further supported by a study by Di Martino et. al [13] which implements machine learning approaches to classify ASD from TD using the same dataset as used in this study (with all sites included). The resulting classification accuracy of approximately 60% is comparable to the study by Di Martino et. al [13].

The study from Di Martino et. al [13] indicated that the main cause of lower classifier performance was due to the intersite variability, which required developing standardized data acquisition protocols. Further, O Artiles et. al [40] studied the effects of confounding factors while developing classifier models post harmonization using rsfMRI functional connectivity resulting with an accuracy of 76.4% with sensitivity and specificity of 82.9% and 77.0% respectively. Similarly, P Dai et. al [41] derived functional connectivity networks to classify depression patients from healthy controls which resulted in an accuracy of 68.9% with sensitivity and specificity of 71.75% and 65.84% respectively post harmonization. Although the current study has a comparably lower performance in terms of sensitivity and specificity despite deriving featureset from functional connectivity, the functional characterization between ASD and TD is more effectively identified through graph theoretical networks. For instance certain subnetworks identified through Louvain modularity measure results in a balanced sensitivity and specificity of 65.22% and 67.92% respectively post harmonization, despite the overall degree centrality tending towards higher specificity.

4.2. Effect of Graph Theoretical Measures in ASD

Graph measures play an important role in distinguishing ASD from TD in terms of their anatomical regions, their functional networks or certain state specific network characteristics S. M. Smith et. al [42]. The Degree centrality (DC) measure tends to decrease in ASD within frontal regions such as the right middle frontal gyrus which correlates with the stereotypic behaviors on ABC scales. Furthermore, another centrality measure called Betweenness centrality shows reduced hubs in regions involving the precuneus and superior temporal gyrus, indicating impaired integration across distant networks, followed by Eigenvector centrality which highlights hypo-centrality in default mode and salience networks, contributing to social cognition deficits, R. M. Thomas et. al [43], A. Kazeminejad and R.C. Sotero [44], A. Abraham et. al [45] and J. D. Power et. al [46]. However, these measures tend to show non-homogenous variability among certain anatomical regions, leading to unstable characterization of network regions in the cerebellar system J. R. Sato

et. al [38]. Although, these characteristics can be influenced by the methodological process, (eg. differences occurring due to head motion with sub-millimeter range, B. T. T. Yeo et. al [47] and J. D. Power et. al [48], they play an important role in the development of complex biomarkers for certain neurological disorders through machine learning frameworks.

4.3. Significance of Machine Learning in Diagnosing ASD using RS-FMRI

The role of machine learning applications in studying the functional connectivity of brain disorders has increased significantly over the last two decades G. Deshpande et. al [9], G. Deshpande et. al [10] and A. A. Chen et. al [12], these models often relied on multiple levels of complexity pertaining to its network characteristics, one such representation involved differentiating ASD from TD through network sparsity of centrality and modularity based measures which was implemented in an earlier study V. K. Raj et. al [56]. Among a wide scope of classifier models, the Support Vector Machine (SVM) based classifier models were identified to be the most prevalent in this case scenario. The significance of this model was further emphasized when we analyzed 93 systematic reviews and 55 meta-analysis studies among which 33 and 27 of those studies had referred to SVM respectively, A. Di Martino et. al [13] and Santana et. al [39]. These studies indicated that SVM and ANN showed a major scope in the implementation of classification models consistently reflecting in 5 or more articles. Among them, the SVM yielded a sensitivity of 76.3% and specificity of 77.5%, which is broadly inline with the results obtained from the current study. One of the major reasons for SVM being the most preferred method as indicated from Santana et. al [39], is due to its ability to generalize, along with addressing noisy, correlated features and high dimensional dataset - factors which play an important role in the current study. A study by D Wen et. al [49] concludes that although issues such as overfitting and sample size exist among both classical machine learning and deep learning techniques. The deep learning techniques may have a comparatively poorer performance under the above circumstances.

One of the limitations of many MRI based studies is that of homogeneity. As indicated earlier, small sample real-world datasets are often acquired from a single site consisting of a homogenous

patient population which makes the process of generalization more difficult while developing a model. Therefore, acquiring samples from multiple acquisition sites enables extraction of robust features which could represent a given pathology. However, a methodological challenge arising from a heterogenous dataset is not trivial, As observed In the current study through fig. 7 and fig. 8, the trend in specificity is contradicting for patients with the same pathology from PITT and KKI with increase in threshold levels. This is due to the limitations from multiple site dataset which cause heterogeneity among sample populations. Further, a reduced sample size of datasource adds to this issue leading to factors causing intersite variability. Therefore, developing harmonization frameworks to reduce intersite variability is an important stage in the development of ML models.

4.4. Effect of MRI Harmonization in ML Models and its Limitations

Studies have shown that machine learning models have helped in distinguishing ASD from Typical Development, J. S. Anderson et. al [50], D. A. Fair et. al [51], M. P. Milham et. al [52] and S. E. Peterson and O. Sporns [53]. As identified by Saponaro et. al [32], the MRI data acquisitions from different scanners, sites and protocols encode certain confounding variables which if not addressed appropriately, may mask the case-control difference K. Zeng et. al [28]. This can be observed in fig. 7 where the specificity with respect to degree centrality and clustering coefficient steadily increases beyond a certain threshold level post harmonization, and the specificity with respect to modularity becomes more stable with increasing threshold value (fig. 8).

However, one of the major limitations of harmonization used in ML models is a phenomenon known as data leakage which occurs when the entire dataset is considered while estimating harmonization parameters M. Rosenblatt et. al [54] and R. Pomponio et. al [55]. As a result of estimating batch effects among all participants, such a model leads to induced correlations among participants who were originally non-correlated leading to correlations among each harmonized data point. Such induced correlation exaggerates the classifier model by falsely overestimating its performance. Methods such as efficacy and harmonizer transformers can help improve the data leakage issue caused by the harmonization process during the development of classifier models R.

Pomponio et. al [55].

5. CONCLUSION

The study shows that harmonization of graph theoretic measures such as centrality and modularity measures play an important role in the classifier performance while distinguishing patients of ASD from TD. While the accuracy of site specific classifier models remained similar, the sensitivity of KKI sites improved post harmonization. This improvement was observed consistently across degree centrality, clustering coefficient and Louvain modularity measures. However, there are limitations in the harmonization process which could affect the classifier's performance through inducing correlation among participants which were independent before leading to data leakage. Factors such as integrating more clinical variables, graph theoretic measures and development of efficient deep learning frameworks would help significantly in addressing this issue.

CONFLICT OF INTERESTS

The authors declare that there is no conflict of interests.

REFERENCES

[1] S. Qiu, Y. Lu, Y. Li, J. Shi, H. Cui, et al., Prevalence of Autism Spectrum Disorder in Asia: A Systematic Review and Meta-Analysis, Psychiatry Res. 284 (2020), 112679. https://doi.org/10.1016/j.psychres.2019.112679.

[2] N. Salari, S. Rasoulpoor, S. Rasoulpoor, S. Shohaimi, S. Jafarpour, et al., The Global Prevalence of Autism Spectrum Disorder: A Comprehensive Systematic Review and Meta-Analysis, Ital. J. Pediatr. 48 (2022), 112. https://doi.org/10.1186/s13052-022-01310-w.

[3] F.V. Farahani, W. Karwowski, N.R. Lighthall, Application of Graph Theory for Identifying Connectivity Patterns in Human Brain Networks: A Systematic Review, Front. Neurosci. 13 (2019), 585. https://doi.org/10.3389/fnins.2019.00585.

[4] M.A. Just, V.L. Cherkassky, A. Buchweitz, T.A. Keller, T.M. Mitchell, Identifying Autism from Neural Representations of Social Interactions: Neurocognitive Markers of Autism, PLoS ONE 9 (2014), e113879. https://doi.org/10.1371/journal.pone.0113879.

[5] L. Borràs-Ferrís, Ú. Pérez-Ramírez, D. Moratal, Link-Level Functional Connectivity Neuroalterations in Autism Spectrum Disorder: A Developmental Resting-State fMRI Study, Diagnostics 9 (2019), 32.

https://doi.org/10.3390/diagnostics9010032.

[6] H. Haghighat, M. Mirzarezaee, B.N. Araabi, A. Khadem, Functional Networks Abnormalities in Autism Spectrum Disorder: Age-Related Hypo and Hyper Connectivity, Brain Topogr. 34 (2021), 306-322. https://doi.org/10.1007/s10548-021-00831-7.

[7] J. Xu, H. Wang, L. Zhang, Z. Xu, T. Li, et al., Both Hypo-Connectivity and Hyper-Connectivity of the Insular Subregions Associated with Severity in Children with Autism Spectrum Disorders, Front. Neurosci. 12 (2018), 234. https://doi.org/10.3389/fnins.2018.00234.

[8] Z. Khandan Khadem-Reza, M.A. Shahram, H. Zare, Altered Resting-State Functional Connectivity of the Brain in Children with Autism Spectrum Disorder, Radiol. Phys. Technol. 16 (2023), 284-291. https://doi.org/10.1007/s12194-023-00717-2.

[9] G. Deshpande, L.E. Libero, K.R. Sreenivasan, H.D. Deshpande, R.K. Kana, Identification of Neural Connectivity Signatures of Autism Using Machine Learning, Front. Hum. Neurosci. 7 (2013), 670. https://doi.org/10.3389/fnhum.2013.00670.

[10] G. Deshpande, Z. Li, P. Santhanam, C.D. Coles, M.E. Lynch, et al., Recursive Cluster Elimination Based Support Vector Machine for Disease State Prediction Using Resting State Functional and Effective Brain Connectivity, PLoS ONE 5 (2010), e14277. https://doi.org/10.1371/journal.pone.0014277.

[11] M.K. Belmonte, E.H. Cook, G.M. Anderson, J.L.R. Rubenstein, W.T. Greenough, et al., Autism as a Disorder of Neural Information Processing: Directions for Research and Targets for Therapy, Mol. Psychiatry 9 (2004), 646-663. https://doi.org/10.1038/sj.mp.4001499.

[12] A.A. Chen, D. Srinivasan, R. Pomponio, Y. Fan, I.M. Nasrallah, et al., Harmonizing Functional Connectivity Reduces Scanner Effects in Community Detection, NeuroImage 256 (2022), 119198. https://doi.org/10.1016/j.neuroimage.2022.119198.

[13] A. Di Martino, C.G. Yan, Q. Li, E. Denio, F.X. Castellanos, et al., The Autism Brain Imaging Data Exchange: Towards a Large-Scale Evaluation of the Intrinsic Brain Architecture in Autism, Mol. Psychiatry 19 (2013), 659-667. https://doi.org/10.1038/mp.2013.78.

[14] Y. Du, Z. Fu, V.D. Calhoun, Classification and Prediction of Brain Disorders Using Functional Connectivity: Promising but Challenging, Front. Neurosci. 12 (2018), 525. https://doi.org/10.3389/fnins.2018.00525.

[15] M.N. Hallquist, F.G. Hillary, Graph Theory Approaches to Functional Network Organization in Brain Disorders: A Critique for a Brave New Small-World, Netw. Neurosci. 3 (2019), 1-26. https://doi.org/10.1162/netn_a_00054.

[16] R.K. Kana, L.Q. Uddin, T. Kenet, D. Chugani, R.A. MÃ¼ller, Brain Connectivity in Autism, Front. Hum. Neurosci. 8 (2014), 349. https://doi.org/10.3389/fnhum.2014.00349.

[17] A. Khazaee, A. Ebrahimzadeh, A. Babajani-Feremi, Classification of Patients with MCI and AD from Healthy

Controls Using Directed Graph Measures of Resting-State fMRI, Behav. Brain Res. 322 (2017), 339-350. https://doi.org/10.1016/j.bbr.2016.06.043.

[18] N. Masuda, M. Sakaki, T. Ezaki, T. Watanabe, Clustering Coefficients for Correlation Networks, Front. Neuroinformatics 12 (2018), 7. https://doi.org/10.3389/fninf.2018.00007.

[19] D. Meunier, R. Lambiotte, E.T. Bullmore, Modular and Hierarchically Modular Organization of Brain Networks, Front. Neurosci. 4 (2010), 200. https://doi.org/10.3389/fnins.2010.00200.

[20] M.E.J. Newman, Modularity and Community Structure in Networks, Proc. Natl. Acad. Sci. 103 (2006), 8577-8582. https://doi.org/10.1073/pnas.0601602103.

[21] M.E.J. Newman, M. Girvan, Finding and Evaluating Community Structure in Networks, Phys. Rev. E 69 (2004), 026113. https://doi.org/10.1103/PhysRevE.69.026113.

[22] K. Qin, D. Lei, W.H. Pinaya, N. Pan, W. Li, et al., Using Graph Convolutional Network to Characterize Individuals with Major Depressive Disorder Across Multiple Imaging Sites, EBioMedicine 78 (2022), 103977. https://doi.org/10.1016/j.ebiom.2022.103977.

[23] K. Rajamanickam, A Mini Review on Different Methods of Functional-Mri Data Analysis, Arch. Intern. Med. Res. 03 (2020), 44-60. https://doi.org/10.26502/aimr.0022.

[24] E. Redcay, J.M. Moran, P.L. Mavros, H. Tager-Flusberg, J.D.E. Gabrieli, et al., Intrinsic Functional Network Organization in High-Functioning Adolescents with Autism Spectrum Disorder, Front. Hum. Neurosci. 7 (2013), 573. https://doi.org/10.3389/fnhum.2013.00573.

[25] S. Hiwa, S. Obuchi, T. Hiroyasu, Automated Extraction of Human Functional Brain Network Properties Associated with Working Memory Load Through a Machine Learning-Based Feature Selection Algorithm, Comput. Intell. Neurosci. 2018 (2018), 4835676. https://doi.org/10.1155/2018/4835676.

[26] N. Tzourio-Mazoyer, B. Landeau, D. Papathanassiou, F. Crivello, O. Etard, et al., Automated Anatomical Labeling of Activations in SPM Using a Macroscopic Anatomical Parcellation of the MNI MRI Single-Subject Brain, NeuroImage 15 (2002), 273-289. https://doi.org/10.1006/nimg.2001.0978.

[27] J.P. Onnela, K. Kaski, J. Kertész, Clustering and Information in Correlation Based Financial Networks, Eur. Phys. J. B - Condens. Matter 38 (2004), 353-362. https://doi.org/10.1140/epjb/e2004-00128-7.

[28] K. Zeng, J. Kang, G. Ouyang, J. Li, J. Han, et al., Disrupted Brain Network in Children with Autism Spectrum Disorder, Sci. Rep. 7 (2017), 16253. https://doi.org/10.1038/s41598-017-16440-z.

[29] M. Rubinov, O. Sporns, Complex Network Measures of Brain Connectivity: Uses and Interpretations, NeuroImage 52 (2010), 1059-1069. https://doi.org/10.1016/j.neuroimage.2009.10.003.

[30] O. Sporns, G. Tononi, R. Kötter, The Human Connectome: A Structural Description of the Human Brain, PLoS Comput. Biol. 1 (2005), e42. https://doi.org/10.1371/journal.pcbi.0010042.

[31] V.D. Blondel, J.L. Guillaume, R. Lambiotte, E. Lefebvre, Fast Unfolding of Communities in Large Networks, J.

Stat. Mech.: Theory Exp. 2008 (2008), P10008. https://doi.org/10.1088/1742-5468/2008/10/P10008.

[32] S. Saponaro, A. Giuliano, R. Bellotti, A. Lombardi, S. Tangaro, et al., Multi-Site Harmonization of MRI Data Uncovers Machine-Learning Discrimination Capability in Barely Separable Populations: An Example from the ABIDE Dataset, NeuroImage: Clinical 35 (2022), 103082. https://doi.org/10.1016/j.nicl.2022.103082.

[33] M.E. Torbati, D.S. Minhas, G. Ahmad, E.E. O'Connor, J. Muschelli, et al., A Multi-Scanner Neuroimaging Data Harmonization Using RAVEL and ComBat, NeuroImage 245 (2021), 118703. https://doi.org/10.1016/j.neuroimage.2021.118703.

[34] L.Q. Uddin, K. Supekar, V. Menon, Reconceptualizing Functional Brain Connectivity in Autism from a Developmental Perspective, Front. Hum. Neurosci. 7 (2013), 343–352. https://doi.org/10.3389/fnhum.2013.00458.

[35] J. Rudie, J. Brown, D. Beck-Pancer, L. Hernandez, E. Dennis, et al., Altered Functional and Structural Brain Network Organization in Autism, NeuroImage: Clinical 2 (2013), 79-94. https://doi.org/10.1016/j.nicl.2012.11.006.

[36] D.S. Bassett, E. Bullmore, Small-World Brain Networks, Neuroscientist 12 (2006), 512-523. https://doi.org/10.1177/1073858406293182.

[37] S. Achard, E. Bullmore, Efficiency and Cost of Economical Brain Functional Networks, PLoS Comput. Biol. 3 (2007), e17. https://doi.org/10.1371/journal.pcbi.0030017.

[38] J.R. Sato, M. Calebe Vidal, S. de Siqueira Santos, K. Brauer Massirer, A. Fujita, Complex Network Measures in Autism Spectrum Disorders, IEEE/ACM Trans. Comput. Biol. Bioinform. 15 (2018), 581-587. https://doi.org/10.1109/TCBB.2015.2476787.

[39] C.P. Santana, E.A. de Carvalho, I.D. Rodrigues, G.S. Bastos, A.D. de Souza, et al., rs-fMRI and Machine Learning for ASD Diagnosis: A Systematic Review and Meta-Analysis, Sci. Rep. 12 (2022), 6030. https://doi.org/10.1038/s41598-022-09821-6.

[40] O. Artiles, Z. Al Masry, F. Saeed, Confounding Effects on the Performance of Machine Learning Analysis of Static Functional Connectivity Computed from rs-fMRI Multi-Site Data, Neuroinformatics 21 (2023), 651-668. https://doi.org/10.1007/s12021-023-09639-1.

[41] P. Dai, T. Xiong, X. Zhou, Y. Ou, Y. Li, et al., The Alterations of Brain Functional Connectivity Networks in Major Depressive Disorder Detected by Machine Learning Through Multisite rs-fMRI Data, Behav. Brain Res. 435 (2022), 114058. https://doi.org/10.1016/j.bbr.2022.114058.

[42] S.M. Smith, P.T. Fox, K.L. Miller, D.C. Glahn, P.M. Fox, et al., Correspondence of the Brain's Functional Architecture during Activation and Rest, Proc. Natl. Acad. Sci. 106 (2009), 13040-13045. https://doi.org/10.1073/pnas.0905267106.

[43] R.M. Thomas, S. Gallo, L. Cerliani, P. Zhutovsky, A. El-Gazzar, et al., Classifying Autism Spectrum Disorder

Using the Temporal Statistics of Resting-State Functional MRI Data with 3D Convolutional Neural Networks, Front. Psychiatry 11 (2020), 440. https://doi.org/10.3389/fpsyt.2020.00440.

[44] A. Kazeminejad, R.C. Sotero, Topological Properties of Resting-State fMRI Functional Networks Improve Machine Learning-Based Autism Classification, Front. Neurosci. 12 (2019), 1018. https://doi.org/10.3389/fnins.2018.01018.

[45] A. Abraham, M.P. Milham, A. Di Martino, R.C. Craddock, D. Samaras, et al., Deriving Reproducible Biomarkers from Multi-Site Resting-State Data: An Autism-Based Example, NeuroImage 147 (2017), 736-745. https://doi.org/10.1016/j.neuroimage.2016.10.045.

[46] S. Xu, M. Li, C. Yang, X. Fang, M. Ye, et al., Abnormal Degree Centrality in Children with Low-Function Autism Spectrum Disorders: A Sleeping-State Functional Magnetic Resonance Imaging Study, Neuropsychiatr. Dis. Treat. 18 (2022), 1363-1374. https://doi.org/10.2147/NDT.S367104.

[47] B.T. Thomas Yeo, F.M. Krienen, J. Sepulcre, M.R. Sabuncu, D. Lashkari, et al., The Organization of the Human Cerebral Cortex Estimated by Intrinsic Functional Connectivity, J. Neurophysiol. 106 (2011), 1125-1165. https://doi.org/10.1152/jn.00338.2011.

[48] J.D. Power, A.L. Cohen, S.M. Nelson, G.S. Wig, K.A. Barnes, et al., Functional Network Organization of the Human Brain, Neuron 72 (2011), 665-678. https://doi.org/10.1016/j.neuron.2011.09.006.

[49] D. Wen, Z. Wei, Y. Zhou, G. Li, X. Zhang, et al., Deep Learning Methods to Process fMRI Data and Their Application in the Diagnosis of Cognitive Impairment: A Brief Overview and Our Opinion, Front. Neuroinformatics 12 (2018), 23. https://doi.org/10.3389/fninf.2018.00023.

[50] J.S. Anderson, J.A. Nielsen, A.L. Froehlich, M.B. DuBray, et al., Functional Connectivity Magnetic Resonance Imaging Classification of Autism, Brain 134 (2011), 3742-3754. https://doi.org/10.1093/brain/awr263.

[51] D.A. Fair, A.L. Cohen, J.D. Power, N.U.F. Dosenbach, J.A. Church, et al., Functional Brain Networks Develop from a “Local to Distributed” Organization, PLoS Comput. Biol. 5 (2009), e1000381. https://doi.org/10.1371/journal.pcbi.1000381.

[52] M.P. Milham, L. Ai, B. Koo, T. Xu, C. Amiez, et al., An Open Resource for Non-Human Primate Imaging, Neuron 100 (2018), 61-74.e2. https://doi.org/10.1016/j.neuron.2018.08.039.

[53] S.E. Petersen, O. Sporns, Brain Networks and Cognitive Architectures, Neuron 88 (2015), 207-219. https://doi.org/10.1016/j.neuron.2015.09.027.

[54] M. Rosenblatt, L. Tejavibulya, R. Jiang, S. Noble, D. Scheinost, Data Leakage Inflates Prediction Performance in Connectome-Based Machine Learning Models, Nat. Commun. 15 (2024), 1829. https://doi.org/10.1038/s41467-024-46150-w.

[55] R. Pomponio, G. Erus, M. Habes, J. Doshi, D. Srinivasan, E. Mamourian, V. Bashyam, I. M. Nasrallah, T. D. Satterthwaite, Y. Fan, L. J. Launer, C. L. Masters, P. Maruff, C. Zhuo, H. Völzke, S. C. Johnson, J. Fripp, N.

Koutsouleris, D. H. Wolf, R. Gur, C. Davatzikos, Harmonization of large MRI datasets for the analysis of brain imaging patterns throughout the lifespan, NeuroImage 208 (2020), 116450. https://doi.org/10.1016/j.neuroimage.2019.116450.

[56] V.K. Raj, A.J. Thomas, Effect of Network Sparsity in Classifier Performance in ASD Patients: A Multicenter Study Based on Centrality Measures of rsfMRI, in: J. Kakarla, R. Balasubramanian, S. Murala, S.K. Vipparthi, D. Gupta, (eds) Computer Vision and Image Processing, Communications in Computer and Information Science, Vol 2474, Springer, Cham, (2026). https://doi.org/10.1007/978-3-031-93691-3_8.

[57] M. Yu, K. A. Linn, P. A. Cook, M. L. Phillips, M. McInnis, M. Fava, M. H. Trivedi, M. M. Weissman, R. T. Shinohara, and Y. I. Sheline, Statistical harmonization corrects site effects in functional connectivity measurements from multi-site fMRI data, Hum. Brain Mapp. 39 (2018), no. 11, 4213–4227. https://doi.org/10.1002/hbm.24241.